

AD A109408

Technical Report
SMU-EE-TR-82 - 1
Contract Number N00014-79-C-0494
January 4, 1982

①
LEVEL II

A Study of Texture
Classification Using Spectral Features*

(1) 16

DTIC FILE COPY

Accession For	
NTIS GRA&I	<input checked="" type="checkbox"/>
DTIC TAB	<input type="checkbox"/>
Unannounced	<input type="checkbox"/>
Justification	
By	
Distribution/	
Availability Codes	
Dist	Avail and/or Special
A	

BY
C. H. Chen
Gia-Kinh Young
Department of Electrical Engineering
Southeastern Massachusetts University
North Dartmouth, Massachusetts 02747

DTIC
ELECTE
S JAN 7 1982 **D**

*The support of the Statistics and Probability Program of the Office of Naval Research on this work is gratefully acknowledged.

DISTRIBUTION STATEMENT A

Approved for public release
Distribution Unlimited

82 01 07 030

407932

AK

A Study of Texture Classification Using Spectral Features

I. Introduction

To identify objects or region of interest in an image, textural properties are very important because of their useful information about the structural arrangement of surfaces and their relationship to the surrounding environment. Various methods of textural feature selection have been proposed (see e.g. [1][2]). Also the spectral information has been generally recognized as an effective feature on the texture discrimination and segmentation. A busy picture has relatively high power at high spatial frequencies as compared to a smooth picture, while the directional biases in the picture should give rise to the directional biases in the spectrum. And any periodic properties should produce very high values in the power spectrum.

Weszka et al. [3] have used this kind of feature for the classification of various terrains. Because of the method used to calculate the power spectrum (taking a two-dimensional Fourier Transform) cannot lead to a satisfactory result for a finite sample two-dimensional data (image), the classification is not as good as using other methods. Recently, Lim and Malik [4] have proposed an efficient iterative algorithm for the two-dimensional maximum entropy power spectrum estimation which can obtain good resolution and sufficient accuracy for the finite sample two-dimensional data. A study of the spectral estimation of texture image has been proved to be successful [5] by using a minicomputer. In this report, we use this method for the calculation of spectral features of texture image. In section II, we will briefly discuss the two-dimensional maximum entropy

power spectrum estimation. The method of selection of features will be described in section III while section IV provides some experimental results of the textural classification.

II. Two-Dimensional Maximum Entropy Power Spectrum Estimation

The basic concept of the maximum entropy method (MEM) of spectral estimation is to extrapolate the autocorrelation function of a random process by maximizing the entropy H of the corresponding probability density function

$$H = \int_{w_1=-\pi}^{\pi} \int_{w_2=-\pi}^{\pi} \log \hat{P}_x(w_1, w_2) dw_1 dw_2 \quad (1)$$

where $\hat{P}_x(w_1, w_2)$ is the power spectrum estimate of the random process $x(n_1, n_2)$. The characteristics of this method are equivalent to the autoregressive signal modeling and the power spectrum is calculated by

$$\hat{P}_x(w_1, w_2) = \frac{1}{\sum_{(n_1, n_2) \in A} \lambda(n_1, n_2) e^{-jw_1 n_1} e^{-jw_2 n_2}} \quad (2)$$

where $\lambda(n_1, n_2)$ is the autocorrelation whose power spectrum is $\frac{1}{\hat{P}_x(w_1, w_2)}$ and A is a set of points (n_1, n_2) where the autocorrelation is known.

Since the filter coefficients cannot be obtained directly by solving the normal equation as in the one-dimensional case, Lim and Malik developed a new iterative algorithm, using adaptive filtering concepts. The basic idea of this algorithm is on the notion that the given correlation point in region A is consistent and the corresponding coefficient should be zero outside region A and proceed this iteration repeatedly until an optimal solution is obtained. That is, for a given autocorrelation $R_x(n_1, n_2)$ for $(n_1, n_2) \in A$, determine $\hat{P}_x(w_1, w_2)$ such that $\hat{P}_x(w_1, w_2)$ satisfy (2) and

$$R_x(n_1, n_2) = F^{-1} \left[P_x(w_1, w_2) \right] \text{ for } (n_1, n_2) \in A$$

A simple flowchart is shown in Fig. 1. We begin with some initial estimate of $\lambda(n_1, n_2)$, obtain the corresponding correlation function, correct the resulting correlation function for $(n_1, n_2) \in A$ with the known $R_x(n_1, n_2)$, obtain the corresponding $\lambda(n_1, n_2)$ from the correct correlation function, and then replace the resulting $\lambda(n_1, n_2)$ with zero for $(n_1, n_2) \notin A$. This completes one iteration and the corrected $\lambda(n_1, n_2)$ is a new estimate of $\lambda(n_1, n_2)$.

In Lim and Malik's paper, the calculation of the autocorrelation $R_x(n_1, n_2)$ is limited to the closed analytic form especially for the two-dimensional sinusoids. A generalization of this method and the application to a two-dimensional real data have been discussed by Chen and Young [5]. To show that this algorithm can fully predict the correct spectrum, an example is to test a three-frequency case. Given a two-dimensional sinusoid whose frequency components are:

	$w_{i1}/2\pi$	$w_{i2}/2\pi$
1)	0.3750	0.1250
2)	0.4375	0.2500
3)	0.0625	0.3750

We can verify from the result shown in Fig. 2 that this algorithm provides a very good spectral estimation and resolution for the multifrequency signal.

III. Feature Selection and Classification Method

We use two features to classify the texture images. It is generally recognized that a coarse texture will have a high value of power spectrum near the origin while in a fine texture, the

value will be more spread out. Thus, if one wishes to analyze texture coarseness, a set of features that should be useful are the averages of the power-spectrum values taken over a ring-shaped region centered at the origin. In this report, we consider only the first quadrant of the power spectrum, then

$$\phi_r = \int_0^{\pi/2} \hat{P}_x(r, \theta) d\theta \quad (3)$$

for various values of r , the ring radius.

For the discrete case, this can be written as (for rings between radius r_1 and r_2):

$$\phi_{r_1 r_2} = \sum_{r_1 \leq x^2 + y^2 \leq r_2} \hat{P}_x(x, y) ; \quad 0 \leq x, y \leq n-1 \quad (4)$$

Similarly, it is well known also that the angular distribution of power spectrum is sensitive to the directionality of the texture in frequency w . A texture with many edges or lines in a given direction θ will have high values of power spectrum around the perpendicular of $\theta + \frac{\pi}{2}$; while in a nondirectional texture the spectrum should also be nondirectional. Thus a good set of features for analyzing the texture directionality should be the averages of the power-spectrum values taken over wedge-shaped regions centered at the origin, i.e.

$$\phi_\theta = \int_0^\infty \hat{P}_x(r, \theta) dr \quad (5)$$

for the various values of θ , the wedge slope.

For the discrete case, this is (the wedge between θ_1 and θ_2) given by

$$\phi_{\theta_1 \theta_2} = \sum_{\substack{\theta_1 \leq \tan^{-1} \frac{y}{x} < \theta_2 \\ 0 \leq x, y \leq n-1}} \hat{P}_x(x, y) \quad (6)$$

The features calculated by (4) and (6) are sensitive to size and orientation respectively, but not to both. In order to obtain the comparable feature sets, we obtain a sets of equalized features by

taking the average over the intersection area of rings and wedges. These equalized features are also studied in section IV.

After the calculation of features, we use the Fisher discriminant technique as the means for classification [6]. For a two-class problem, a given set of features measured x , we decide it belongs to class 1 (subset H_1), if

$$w^t(x - m) > 0 \quad (7)$$

Otherwise we decide class 2 (subset H_2) and,

$$w = \alpha n S_w^{-1}(m_1 - m_2) \quad (8)$$

where

α : a scalar

n : number of samples

S_w : the pooled sample scatter matrix = $\sum_{i=1}^2 \sum_{x \in H_i} (x - m_i)(x - m_i)^t$

m_i : mean = $\frac{1}{n_i} \sum_{x \in H_i} x$, $i=1,2$.

When we have more than two classes, we can use a voting scheme to classify a given measurement x . For each pair of classes H_i, H_j , we project x on appropriate line and classify it as described above. This gives us $k(k-1)/2$ different classifications, where k is the number of classes of x . Finally, we assign x to the class that received the most votes.

IV. Experimental Results

Because of the computational requirements of the method and the limited memory capacity of the PDP 11/45, all test samples are stored in our DEC 20 system and sent through a high speed communication line to the PDP 11/45 for the spectrum computation. The test samples are the texture images taken from the USC data base. To

verify the sensitivity both in coarseness and directionality, we select some textures that contain such informations. The test samples contain six classes of texture (each one has four samples) and are shown in Fig. 3. Each data is a 32×32 array of gray level 0 - 255. These pictures reappear but are two times larger in Fig. 4(a) - Fig. 9(a). Fig. 4(b) - Fig. 9(b) are the corresponding estimated power-spectrum display of the upper left data in each class. We can see that those spectra are different either in radial or angular distribution.

The feature sets we used are:

ring: ϕ_{r,r_2} for $(r_1, r_2) = (1,3), (3,6), (6,12), (12,24), (24,48)$
 wedge: ϕ_{θ,θ_2} for $(\theta_1, \theta_2) = (0,15), (15,30), (30,45), (45,60), (60,75), (75,90)$

The maximum ring radius used is 48 since it already covers most part of a 64×64 array power spectrum.

A combination feature of ring and wedge has been tested for 30 pairs of feature values. Table I shows part of features which did higher than 19 out of 24 correct, i.e. more than 80% correct. Table II shows the best performing pairs using the same kind of features (ring and ring, wedge and wedge); there are 6 out of 25 pairs which classified correctly higher than 75%. Other pairs' results are concentrated near 12-17, i.e., more than 50% correct recognition. For the pairs that contain the wedge near the edges, the results are very good since the test samples give some directional information. Also for the rings a little farther from the origin, the results are better since it shows a large difference in the spectrum value there.

Equalized features are also tested: we used five rings intersected with three wedges (ring: (1,3), (3,6), (6,12), (12,24), (24,48) and wedge: (0,30), (30,60), (60,90)). 105 pairs of features have been tested. Table III shows the best performing pairs of which the best score, 23 out of 24, is 95% correct. From the results, we can see that the ring feature (24,48) gives very useful classification information indicating that there exists a large textural variation in that region as the texture coarseness plays an important role in the pair. Fig. 10 is a histogram of scores obtained of all the 105 pairs of test features and indicates a high probability for the overall classification accuracy of the spectral features.

V. Discussion

In this report, we have observed that equalized features did better than unequalized ones for this set of test samples. It is verified that both the coarseness and the directionality are important factors in texture discrimination. For the consideration of practical use in automatic classification, various kinds of textures must be tested and compared with other methods using the non-spectral features. Another important factor which may influence the results is that if we increase the autocorrelation function and the discrete Fourier transform length while estimating the power spectrum, the accuracy and the resolution will be better. But there is a tradeoff between the accuracy and the computational time. In this report, these parameters (i.e. autocorrelation function: 7x7, discrete Fourier transform length: 32) are chosen

for the real-time processing purpose. Also the locations of the main and second components of frequencies can serve as another important features because they vary among different textures.

References

1. R. M. Haralick, K. Shanmugam and I. Dinstein, "Textural features for image classification," IEEE Trans. on Systems, Man and Cybernetics, vol. SMC-3, pp. 610-621, Nov. 1973.
2. C. H. Chen and P. C. Chen, "A comparative evaluation of texture measures," Technical Note No. EE-75-9, SMU, N. Dartmouth, MA Sept. 25, 1975.
3. J. S. Weszka, C. Dyer and A. Rosenfeld, "A comparative study of texture measures for terrain classification," IEEE Trans. on Systems, Man and Cybernetics, vol. SMC-6, pp. 269-285, 1976.
4. J. S. Lim and N. A. Malik, "A new algorithm for two-dimensional maximum entropy power spectral estimation," IEEE Trans. on Acoustics, Speech and Signal Processing, vol. ASSP-29, no. 3, pp. 401-413, June 1981.
5. C. H. Chen and G. K. Young, "On a two-dimensional maximum entropy spectral estimation method for the texture-image analysis," SMU-EE-TR-81-16, Technical Report, SMU, N. Dartmouth, MA, Oct. 1981.
6. R. O. Duda and P. E. Hart, "Pattern Classification and Scene Analysis," Wiley, 1972.

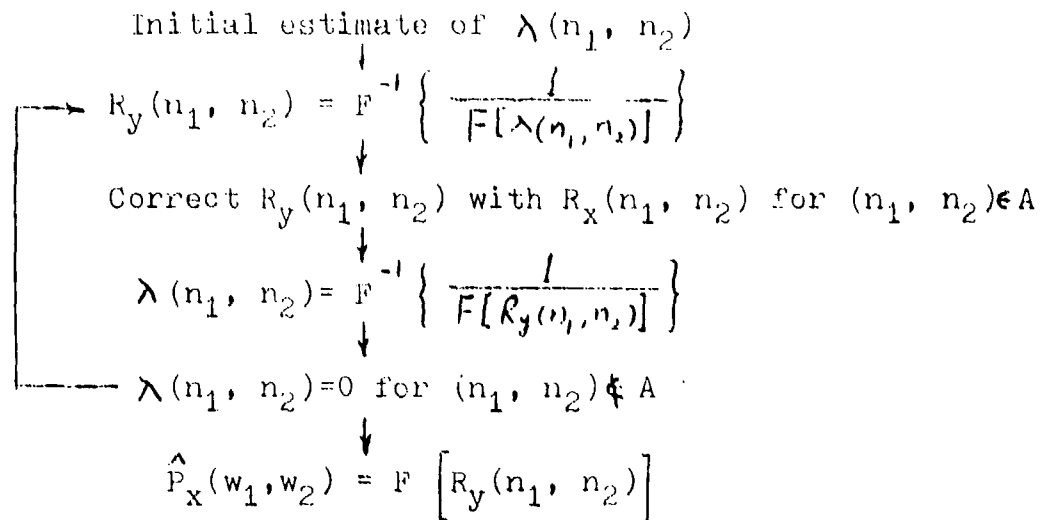


Figure 1

Fig. 2(a) The contour map of the estimated power spectrum ($\Delta \text{dB} = 5$)
Note: ΔdB is the dB value difference between each contour.

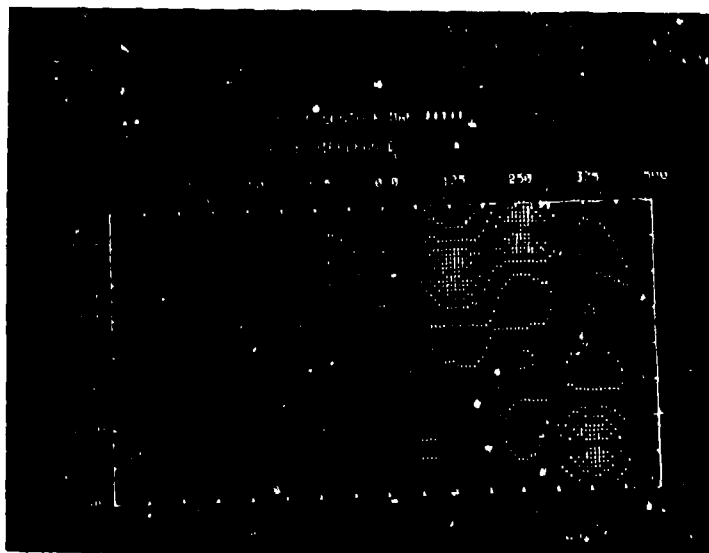
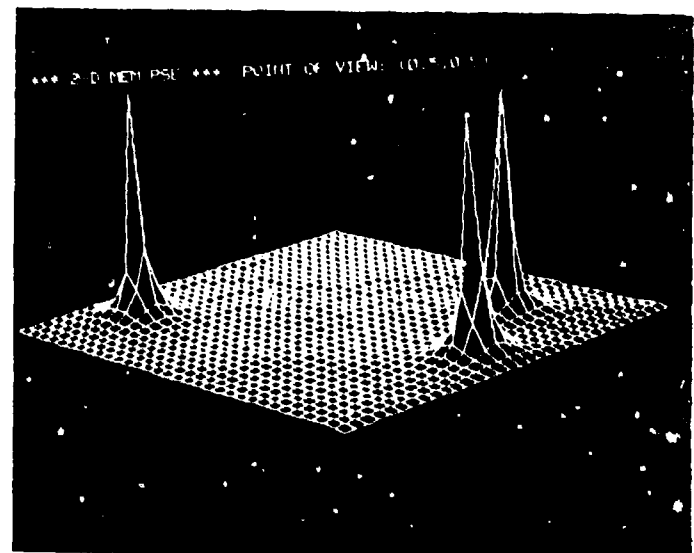


Fig. 2(b) Three-dimensional display of the estimated power spectrum.



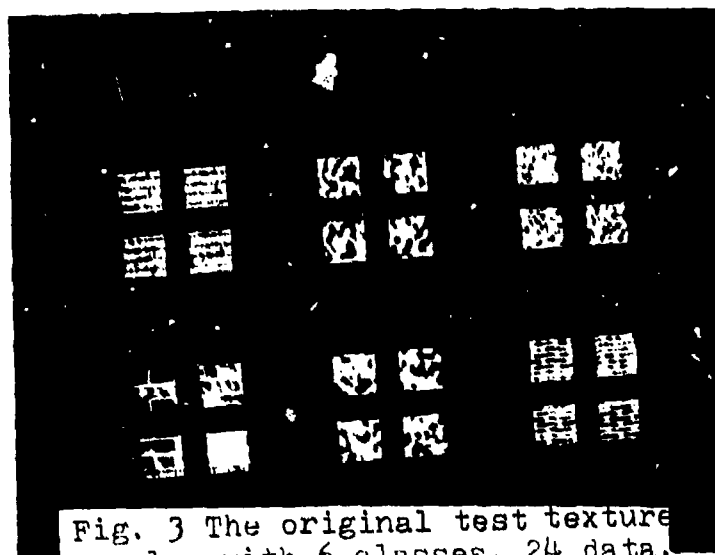


Fig. 3 The original test texture samples with 6 classes, 24 data, and each data format of 32x32.

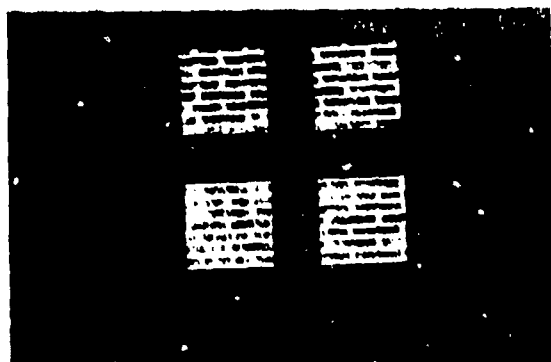


Fig. 4(a) Test samples of class 1.

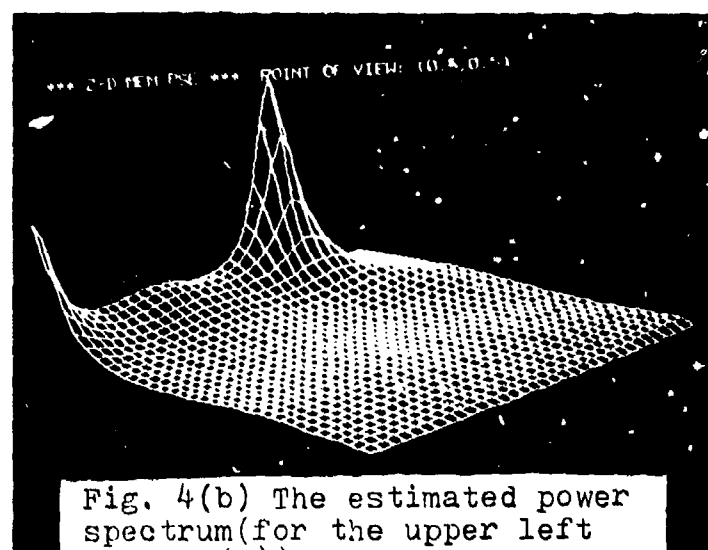


Fig. 4(b) The estimated power spectrum (for the upper left one of (a)).

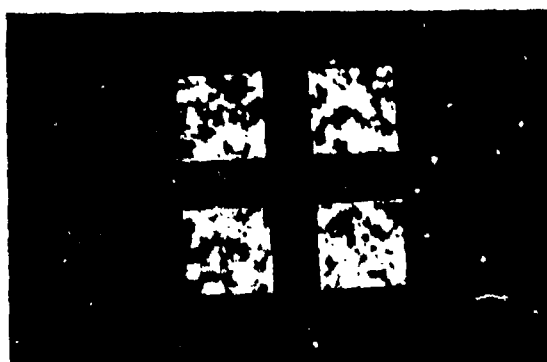


Fig. 5(a) Test samples of class 2.

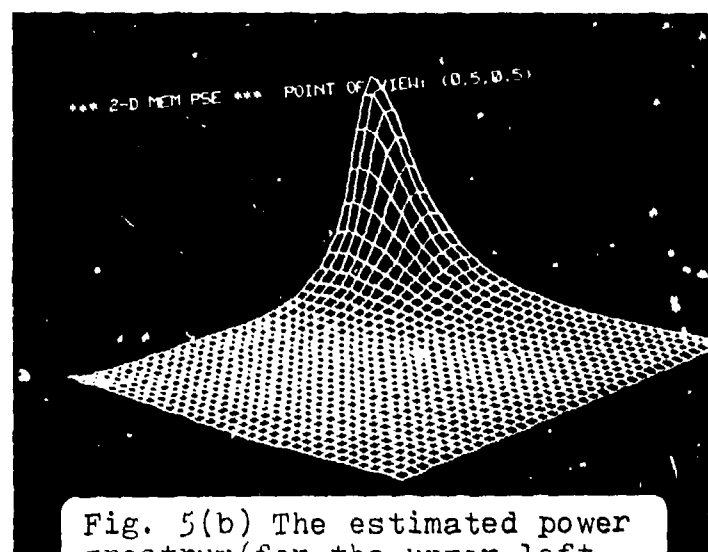


Fig. 5(b) The estimated power spectrum (for the upper left one of (a)).



Fig. 6(a) Test samples of class 3.

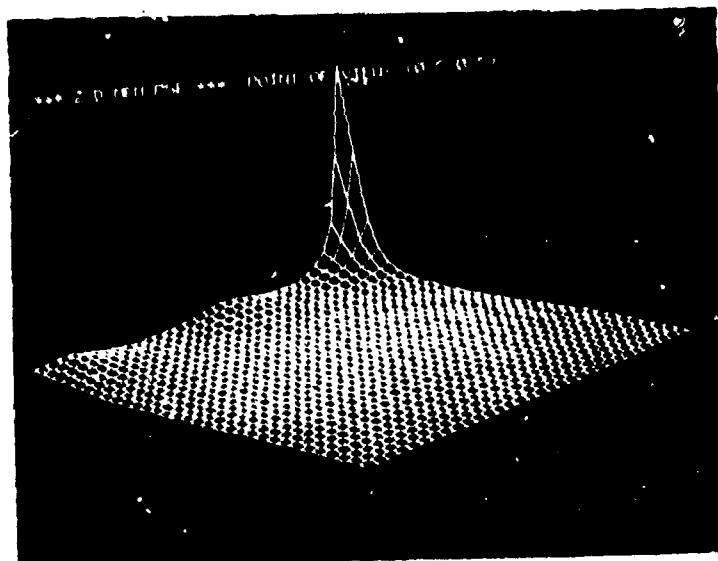


Fig. 6(b) The estimated power spectrum (for the upper left one of (a)).

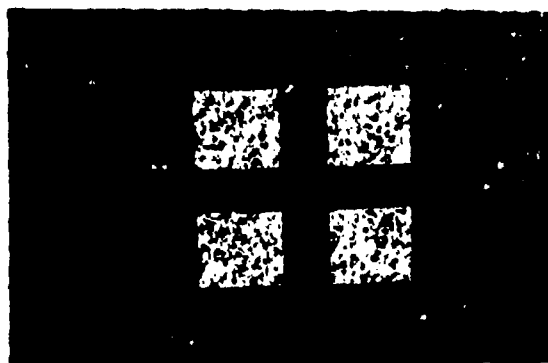


Fig. 7(a) Test samples of class 4.

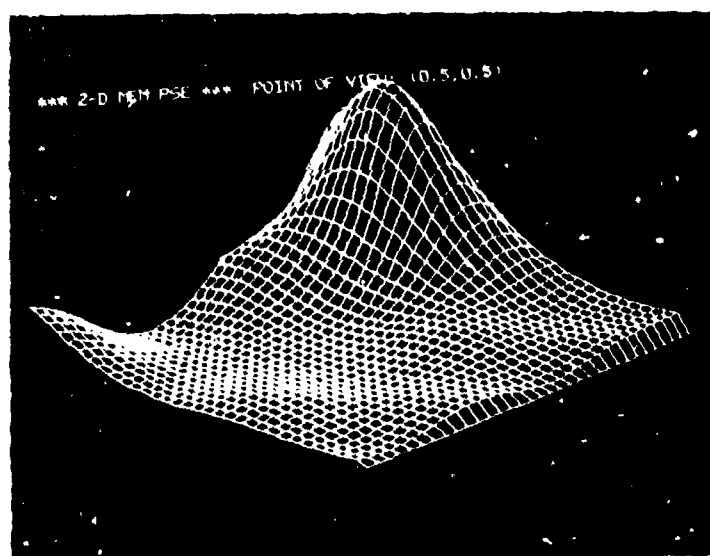


Fig. 7(b) The estimated power spectrum (for the upper left one of (a)).



Fig. 8(a) Test samples of class 5.

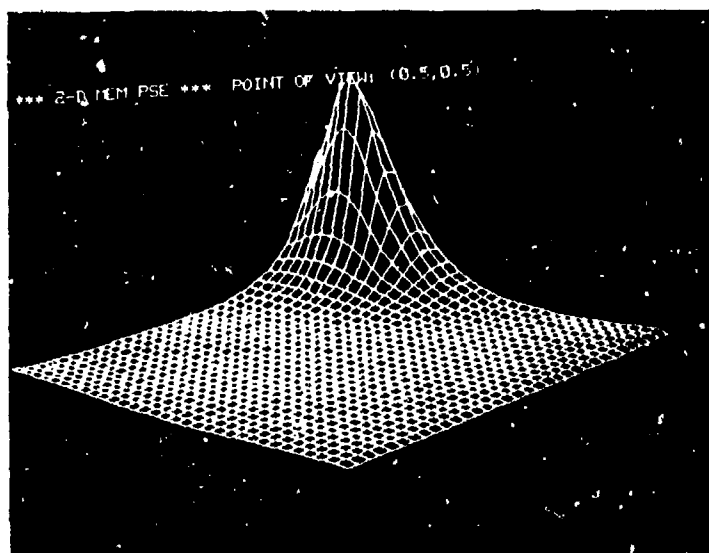


Fig. 8(b) The estimated power spectrum for the upper left one of (a).

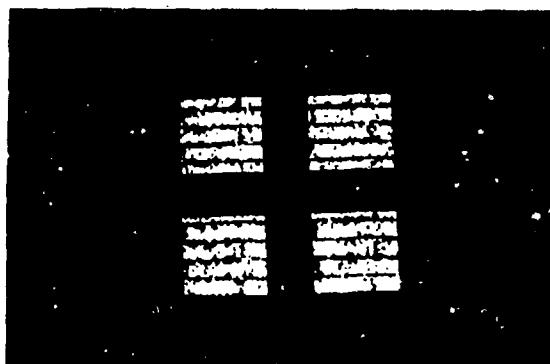


Fig. 9(a) Test samples of class 6

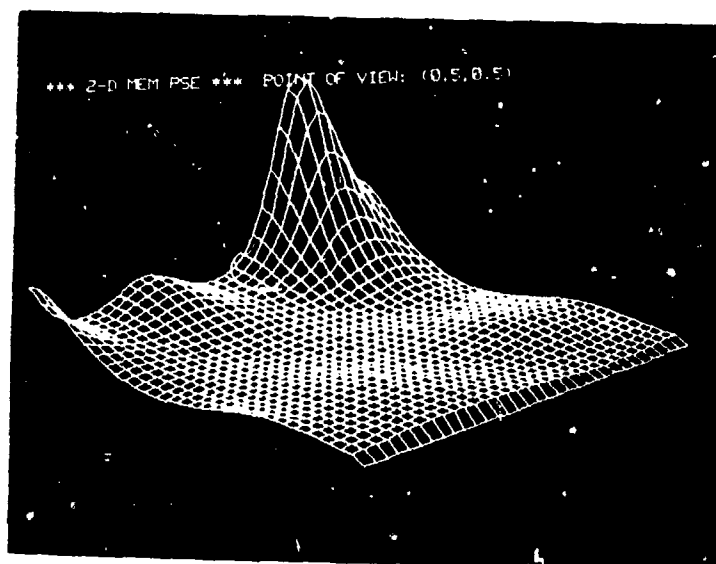


Fig. 9(b) The estimated power spectrum for the upper left one of (a).

Features		Number correctly classified
<u>Ring</u>	<u>Wedge</u>	
(24,48)	(0,15)	22
(1,3)	(0,15)	21
(3,6)	(0,15)	20
(1,3)	(45,60)	19
(12,24)	(0,15)	19
(3,6)	(30,45)	19
(3,6)	(75,90)	19

Table I: Best performing pairs using the combination feature of ring and wedge for those with more than 80% correct classification.

Features		Number correctly classified
<u>Ring</u>	<u>Ring</u>	
(6,12)	(24,48)	20
(6,12)	(12,24)	19
<u>Wedge</u>	<u>Wedge</u>	
(30,45)	(75,90)	20
(15,30)	(60,75)	18
(30,45)	(60,75)	18
(45,60)	(60,75)	18

Table II: Best performing pairs using same kind of features, for those with more than 75% correct classification.

Features				Number correctly classified
Ring	\cap	Wedge	Ring \cap Wedge	
(3,6)		(0,30)	(24,48) (0,30)	23
(12,24)		(60,90)	(24,48) (0,30)	23
(24,48)		(0,30)	(24,48) (30,60)	22
(1,3)		(0,30)	(24,48) (0,30)	22
(1,3)		(30,60)	(24,48) (0,30)	22
(1,3)		(60,90)	(24,48) (0,30)	22
(3,6)		(30,60)	(24,48) (0,30)	21
(3,6)		(60,90)	(24,48) (0,30)	21
(6,12)		(0,30)	(24,48) (0,30)	21
(12,24)		(30,60)	(24,48) (0,30)	21
(12,24)		(0,30)	(12,24) (60,90)	20
(1,3)		(30,60)	(6,12) (0,30)	20
(1,3)		(60,90)	(6,12) (0,30)	20
(12,24)		(0,30)	(24,48) (0,30)	20
(1,3)		(0,30)	(6,12) (0,30)	19
(3,6)		(0,30)	(6,12) (0,30)	19
(3,6)		(30,60)	(6,12) (0,30)	19
(6,12)		(0,30)	(12,24) (60,90)	19

Table III: Best performing pairs using equalized features for those with more than 80% correct classification.

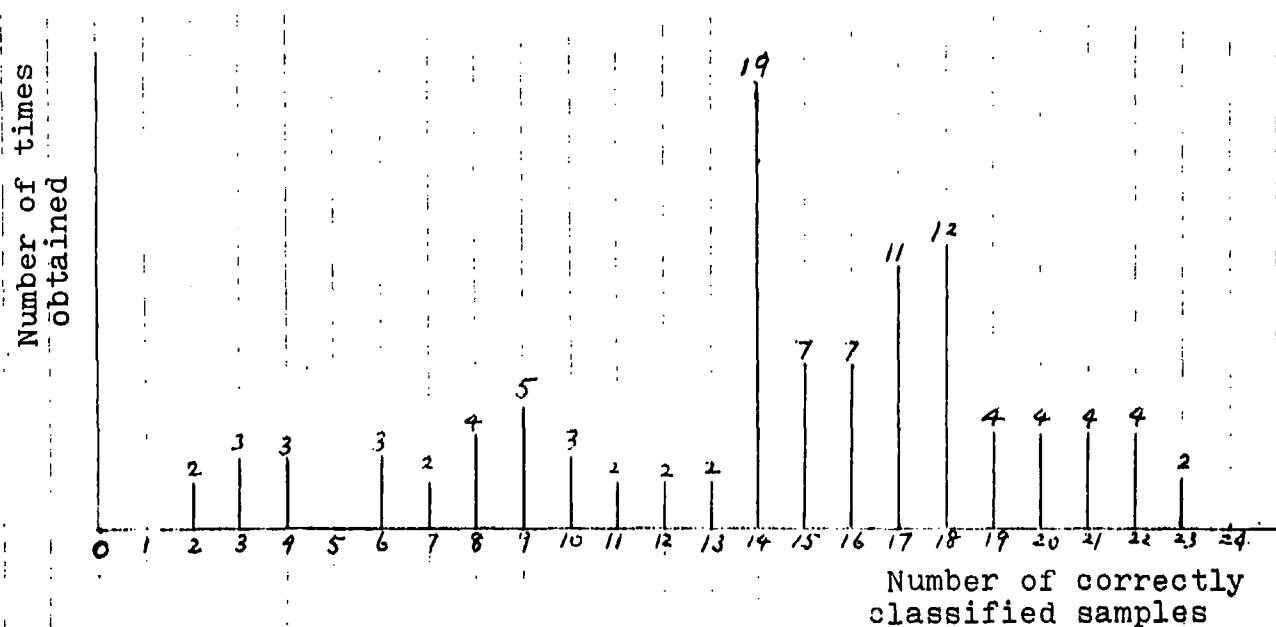


Fig. 10 Histogram of scores obtained using pairs of equalized features

REPORT DOCUMENTATION PAGE		READ INSTRUCTIONS BEFORE COMPLETING FORM
1. REPORT NUMBER	2. GOVT ACCESSION NO.	3. RECIPIENT'S CATALOG NUMBER
	AD-A201 408	
4. TITLE (and Subtitle)	5. TYPE OF REPORT & PERIOD COVERED	
A Study of Texture Classification Using Spectral Features	Technical Report	
6. AUTHOR	7. PERFORMING ORG. REPORT NUMBER	
C. H. Chen and Gia-Kinh Young	SMU-EE-TR-82-1	
8. PERFORMING ORGANIZATION NAME AND ADDRESS	9. CONTRACT OR GRANT NUMBER(s)	
Dept. of Electrical Engineering Southeastern Massachusetts University North Dartmouth, Massachusetts 02747	N00014-79-C-0494	
10. CONTROLLING OFFICE NAME AND ADDRESS	11. REPORT DATE	
Statistics and Probability Program Office of Naval Research, Code 436 Arlington, Virginia 22217	1/4/1982	
12. MONITORING AGENCY NAME & ADDRESS (if different from Controlling Office)	13. NUMBER OF PAGES	
	16	
	14. SECURITY CLASS. (of this report)	
	Unclassified	
	15. DECLASSIFICATION/DOWNGRADING SCHEDULE	
16. DISTRIBUTION STATEMENT (of this Report)		
APPROVED FOR PUBLIC RELEASE: DISTRIBUTION UNLIMITED.		
17. DISTRIBUTION STATEMENT (of the abstract entered in Block 20, if different from Report)		
18. SUPPLEMENTARY NOTES		
19. KEY WORDS (Continue on reverse side if necessary and identify by block number)		
Texture images, 2-D maximum entropy spectral estimation, spectral features, rings and wedges, Fisher's linear discriminant, iterative algorithm, classification performance, finite-size sample, texture coarseness and directionality.		
20. ABSTRACT (Continue on reverse side if necessary and identify by block number)		
Prior spectral feature study was not successful because of inaccuracy in 2-D spectral estimation. In this report, a generalization of Lim-Malik method is used to accurately estimate the ring and wedge spectral features for classification of textural images with a typical performance of over 80 percent correct classification for six texture classes. The results compare favorably with other texture features but require less computation using iterative algorithm.		

DD FORM 1473 1 NOV 65 IS OBSOLETE

Unclassified

SECURITY CLASSIFICATION OF THIS PAGE (When Data Entered)